Antenna Measurements in Reverberation Chambers and Their Relation to Monte Carlo Integration Methods

Robert Rehammar, Anton Skårbratt and Christian Lötbäck-Patané
Bluetest AB
Göteborg, Sweden
Email: firstname.lastname@bluetest.se

***Abstract*—In this paper we point out the similarities between measurements performed in a reverberation chamber and the numerical method of Monte Carlo integration. Further, the corresponding measurements in anechoic chambers will be viewed as Riemann-type of integration.**

The insight that reverberation chamber measurements share many similarities with Monte Carlo integrations is not of pure academic interest. It opens up to utilize many of the methods developed in computational physics and statistics to speed up Monte Carlo integrations. Some of these techniques will be discussed here together with applications.

***Index Terms*—reverberation chamber, OTA, Monte Carlo, variance reduction, antenna testing**

I. Introduction

Mobile antenna measurements can be divided into active and passive measurements. Passive measurements consists of characterizing antennas designed for mobile communication. Typically sought parameters are efficiency and diversity gain. In active measurements, the antenna is integrated in a powered device, such as a smartphone. Total radiated power and total radiated sensitivity are measured and characterize the whole receiver or transmitter chain, including antennas and amplifiers [1] [2] [3], [4].

The antenna diagram plays a central role in both active and passive over-the-air measurements. The antenna diagram is often denoted

$$\bar{G}(\theta,\phi) = \hat{\theta}G_\theta(\theta,\phi) + \hat{\phi}G_\phi(\theta,\phi),$$

where $\bar{G}$ is the complex vector-valued antenna diagram containing information about both θ- and ϕ-polarization via G_θ and G_ϕ. Amplitude and phase of the radiation is captured in the complex values of these functions. However, in the figures of merit listed above, $\bar{G}$ does not figure directly, but rather the integral over $\bar{G}$, or some similar quantity such as:

$$FoM \sim \iint_{4\pi} |\bar{G}|^2 \cdot \mathrm{d}\hat{r}.$$

It is well known that an integral can be computed in a number of different ways, and numerically two common methods are the Riemann-approximation and the Monte Carlo-approximation. Further, the computational techniques of the Riemann approximation will be identified with measurements in the AC, while the Monte Carlo techniques will be identified with measurements in the RC. Applications of these identifications will be discussed.

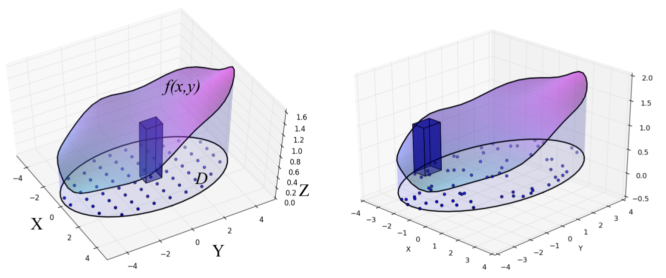

Fig. 1. Example of a region, D, over which I is approximated using a Riemann-sum with a grid indicated by the blue dots (left) and where the corresponding Monte Carlo approximation is used (right). The rectangular block illustrates one volume element, $h_i \cdot f(x_i, y_i)$, in the sum.

In general terms

$$I = \int_D f \,\mathrm{d}x \tag{1}$$

where I denote the integral and f the integrand. The region of integration is denoted by D and the integration measure by $\mathrm{d}x$. We consider the general case where the dimensionality of these quantities is left open and denoted by d, and the function f is a smooth function. If one wishes to evaluate I in equation (1) numerically one can utilize the Riemann approximation which says that

$$I_N^{\text{Riemann}} = \sum_{D_N} h_i \cdot f(x_i) \to I,\, N \to \infty, \tag{2}$$

where D_N denote a regular lattice of D with area elements h_i centered around the x_i points. The approximation is illustrated for a two dimensional case to the left in figure 1.

Another way to compute I in equation (1) is by using the fact that for a random variable, X, with a probability density function $p_X(x)$,

$$I = \int f(x)\mathrm{d}x = \int \frac{f(x)}{p_X(x)} p_X(x)\mathrm{d}x = \mathbb{E}\left[\frac{f(X)}{p_X(X)}\right], \tag{3}$$

where $\mathbb{E}[\cdot]$ denote the expectation.

Let

$$g(x) = \frac{f(x)}{p(x)}.$$

 Copyright (C) 2015 IEICE

An estimate of $E[g(X)]$ is the mean, m. Thus, the integral I can be approximated using

$$I_N^{\text{MC}} = m = \frac{1}{N} \sum_i g(x_i) \tag{4}$$

where x_i are samples from the random variable X. This is illustrated to the right in figure 1. For this to work, $p_X(x) \neq 0 \, \forall x : f(x) \neq 0$ must hold. This method of estimating I is known as the Monte Carlo method [**?**].

A. Convergence

It is well known that the two approximations found in equations (2) and (4) have different convergence speed where the error in I_N^{Riemann} is $O(1/N^{1/d})$ and in I_N^{MC} it is $O(1/\sqrt{N})$ (this is from the standard deviation).

Thus, if the dimensionality of the integral is larger than 2, it is in general beneficial to perform a Monte Carlo integration in favor of a Riemann type of approximation. In the case of antenna measurements, the antenna diagram has the signature

$$\bar{G} : \mathbb{R}^2 \to \mathbb{C}^2,$$

and hence the two methods have the same convergence speed with respect to the number of samples.

II. Antenna measurements

Measurements performed in an anechoic chamber are easily identified with a Riemann type of approximation to the integral and thus this case does not require much analysis. Hence the theory of Riemann integration with e.g. error estimation hold for measurements in an AC directly. The antenna, or device under test is sampled in all directions by rotating it over the whole sphere in fixed steps. By using absorbing material on the chamber walls, only radiation propagating in the line-of-sight between the device under test and a test probe antenna contribute to the transfer function in each rotation state of the device under test. Thus the scenario is very similar to the situation in a Riemann integration.

For the reverberation chamber, on the other hand, the connection is not quite as straight forward. The relation between a measurement in a reverberation chamber and a Monte Carlo integration will be discussed next.

A reverberation chamber consists of a large (in wavelengths) metal cavity and for a specific measurement frequency, many modes are excited in the chamber. The boundary conditions of the cavity are modified in a stochastic manner by moving so called stirrers, which are large metal objects, in the chamber. This generates a transfer function between antennas positioned in the chamber which fluctuates stochastically.

Consider the simplest type of antenna measurement performed in a reverberation chamber, an efficiency measurement. A VNA is connected to the reverberation chamber and the antenna under test is mounted in the chamber according to figure 2. For each stirrer position, the received signal does not correspond to a specific $G(\Theta, \Phi)$, but can rather be modeled as a superposition of several directions so that the received signal in a mode stirrer positions i is

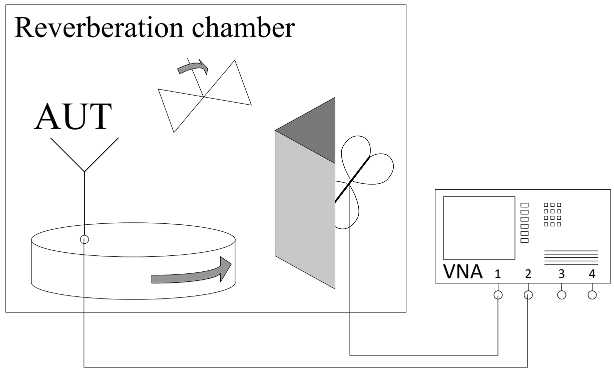

Fig. 2. Set-up for efficiency measurement of an antenna in a reverberation chamber.

$$g_i = \sum_{j=1}^{M^{(i)}} \alpha_{j,\theta}^{(i)} G_\theta(\theta_j^{(i)}, \phi_j^{(i)}) + \alpha_{j,\phi}^{(i)} G_\phi(\theta_j^{(i)}, \phi_j^{(i)}) \tag{5}$$

where $\alpha_{j,\theta|\phi}^{(i)}$, $\theta_j^{(i)}$ and $\phi_j^{(i)}$ are random variables. $M^{(i)}$ denote the number of plane waves excited in the chamber and is related to the number of modes excited. Due to the design of the reverberation chamber (for a well designed chamber with high isotropy) it can be argued that incidence angles should be uniformly distributed over the sphere and hence ϕ_j has a uniform distribution over $(-\pi, \pi]$ and θ_j is distributed according to the probability density function $f(\theta) \sim \sin(\theta)$ for all i and j. The coefficients $\alpha_{j,\theta}$ and $\alpha_{j,\phi}$ are independent identically distributed in a well designed chamber (polarization balanced chamber) and are related to the coupling of the antenna to the modes in the chamber.

The coupling coefficients, α, can be expected to be distributed according to $\arg \alpha \sim U(0, 2\pi)$ and $|\alpha| \sim U(0, L)$, where L is related to the loss in the chamber. This yields $\mathbb{E}(\alpha) = 0$ and $\text{Var}(\alpha) = \mathbb{E}(\alpha\alpha^*) = \frac{2\pi}{3}L$. If the chamber is over-moded as it should be, that is $M^{(i)}$ in equation (5) is large, then via the central limits theorem it can be argued that $g_i \sim \mathcal{CN}(0, \sigma^2)$. Hence $|g_i| \sim \text{Rayleigh}(\sigma)$ and $|g_i|^2 \sim \text{Exp}(1/2\sigma^2)$.

Via a simple computation and linearity of expectation and that cross-terms in equation (5) are IID and has expectation zero it is seen that

$$\begin{aligned} \sigma^2 &= \mathbb{E}(g_i - 0)(g_i - 0)^*) = \\ &= \mathbb{E}(\alpha\alpha^*) \int\int |G_\theta|^2(\theta, \phi) + |G_\phi|^2(\theta, \phi) \sin\theta \mathrm{d}\theta \mathrm{d}\phi = \\ &= \mathbb{E}(\alpha\alpha^*)e \end{aligned}$$

where e denote the antenna efficiency. This is the formula used for computing antenna efficiency from an RC measurement. The term $\mathbb{E}(\alpha\alpha^*)$ is obtained via a so called reference measurement using an antenna with known efficiency.

In greater detail, the convergence speed of the Monte Carlo integration is actually

$$\sqrt{\frac{\sigma^2}{N}} \tag{6}$$

where σ^2 is the variance of the random variable to be sampled. In general one is interested in the relative error. For an exponential distribution, the variance is the same as the expectation and hence can be normalized by the average chamber loss.

In this sense, a measurement in an RC can be identified with an MC integration. The identification is not as straight forward as in the Riemann/AC case due to the sum appearing in equation (5). However, much of the theory applicable to Monte Carlo integration can be applied also on measurements in RCs.

III. Application

The identification developed above can be applied to improve reverberation chamber performance. One such performance improvement is to use the rather large knowledge base that exists in computational Monte Carlo integration to speed up the integration, that is, reduce the required number of samples for the same accuracy.

There are several techniques to make a Monte Carlo integration converge faster, see e.g. [5]. The most well known are the *control variate method*, *importance sampling*, *antithetic variables* and *common random numbers*.

As an example, consider the method of control variate. Here we review the general control variate method, and later apply it to antenna measurements. Let μ denote an unknown parameter of interest and assume that a statistic g with the property $\mathbb{E}(g) = \mu$ is available. Typically samples from g are obtained from computations, but in the case of antenna measurements, it is obtained from the reverberation chamber measurements. Suppose further that there is another statistic $\tilde{g}$ with $\mathbb{E}(\tilde{g}) = \nu$. Then, a new unbiased statistic

$$g^* = g + c(\tilde{g} - \nu)$$

can be constructed with $\mathbb{E}(g^*) = \mu$. The constant c can be any number, but choosing

$$c = -\frac{\mathrm{Cov}(g, \tilde{g})}{\mathrm{Var}(\tilde{g})}$$

minimizes the variance of g^* and hence according to equation (6) will improve the convergence of the estimate.

In the language of reverberation chamber and antenna measurement this correspond to finding a measurement set-up where there is correlation between two antenna measurements. This is often not that easy, but there are interesting cases where it is. One such scenario is when an antenna is being developed in several steps, the first measurement of the efficiency can be imagined to have a high correlation to the second measurement where the antenna prototype will have only minor modifications. This will be particularity true if only the efficiency and not the actual pattern of the antenna is modified.

To demonstrate this, total radiated power was measured on a commercial phone using the Bluetest RTS60 RC. The antenna on the phone was artificially modified to simulate development steps of the antenna. The result can be seen in figure 3. For some cases the method does not improve convergence at all, but for some cases convergence is significantly improved. For

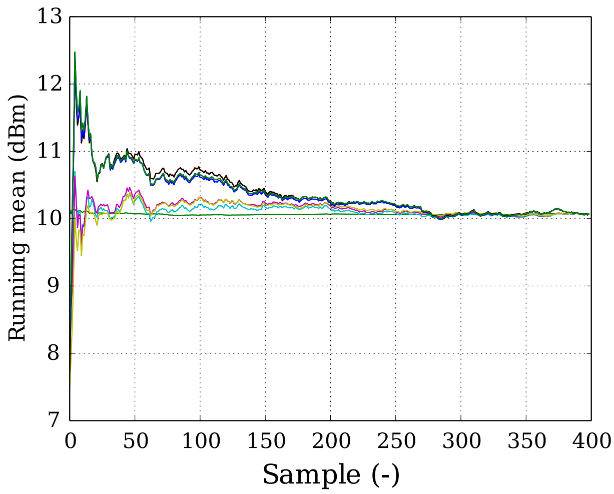

Fig. 3. Result from TRP measurements from 7 different artificial antenna modifications and using the control variate method for improved convergence.

a repeated measurement (green line) the convergence is fast enough to yield the final result after only a few samples.

IV. Conclusion

In this paper it was shown that RC antenna and device measurements can be related to Monte Carlo integration. Using the similarities, it was further shown that techniques developed for Monte Carlo integration can be used to improve convergence speed in RC measurements.

There is a large set of applications when these methods can be used to improve convergence speed. However, it should also be noted that these methods can not be used to improve minimum measurement uncertainty.

References

[1] P.-S. Kildal, X. Chen, C. Orlenius, M. Franzen, and C. Lötbäck-Patané, "Characterization of reverberation chambers for OTA measurements of wireless devices: Physical formulations of channel matrix and new uncertainty formula," vol. 60, no. 8, pp. 3875–3891, 2012.

[2] P.-S. Kildal and K. Rosengren, "Correlation and capacity of MIMO systems and mutual coupling, radiation efficiency, and diversity gain of their antennas: simulations and measurements in a reverberation chamber," vol. 42, no. 12, pp. 104 – 112, 2004.

[3] P. Kildal, A. Hussain, X. Chen, C. Orlenius, A. Skårbratt, J. Åsberg, T. Svensson, and T. Eriksson, "Threshold receiver model for throughput of wireless devices with MIMO and frequency diversity measured in reverberation chamber," vol. 10, pp. 1201–1204, 2011.

[4] P. Kildal, C. Orlenius, and J. Carlsson, "OTA testing in multipath of antennas and wireless devices with MIMO and OFDM," vol. 100, no. 7, pp. 2145–2157, 2012.

[5] C. P. Robert and G. Casella, *Introducing Monte Carlo methods with R*, Springer, 2010.